Vol 14 No 8, August 2005
1009-1963/2005/14(08)/1631-08

Chinese Physics

© 2005 Chin. Phys. Soc.
and IOP Publishing Ltd

Band structures, chemical bonding, and frequency-dependent optical properties of nonlinear optical crystals $HgGa_2S_4$ and $Hg_{0.5}Cd_{0.5}Ga_2S_4$*

Huang Shu-Ping(黄淑萍)†, Wu Dong-Sheng(吴东升), Li Xiao-Dong(李晓东), Lan You-Zhao(蓝尤钊), Zhang Hao(张 浩), Gong Ya-Jing(龚亚京), Li Fei-Fei(李飞飞), Shen Juan(沈 娟), and Cheng Wen-Dan(程文旦)

State Key Laboratory of Structural Chemistry, Fujian Institute of Research on the Structure of Matter, the Graduate School of the Chinese Academy of Sciences, Fuzhou 350002, China

(Received 21 January 2005; revised manuscript received 25 April 2005)

Band structures, density of states, chemical bonding properties, and frequency-dependent linear and nonlinear optical properties have been investigated in terms of the density functional theory and an anharmonic oscillator model for $HgGa_2S_4$ (HGS) and $Hg_{0.5}Cd_{0.5}Ga_2S_4$ (HCGS) crystals. The results obtained show that the top valence bands (VBs) are contributions from Ga–S bonding states and the bottom conduction bands (CBs) are mostly due to Ga–S antibonding states for the HGS crystal, and the top VBs mostly originates from the S-3p states and the bottom CBs are mainly composed of the Ga–S antibonding states for the crystal HCGS. The population analysis shows that both crystals have mixed ionic-covalent bonds. The interactions between Ga and S atoms mostly appear as covalent character, and the Hg–S and Cd–S bonds have substantially ionic characters in HGS and HCGS crystals, respectively. The calculated refractive indices of HGS are compared with the experimental ones, and are found to be in agreement with the experiment data in the low-energy region. It is also found that the band gap of HGS is smaller than that of HCGS, and that the second-order susceptibilities of HGS are larger than those of HCGS.

Keywords: electronic structure, optical properties, $HgGa_2S_4$, $Hg_{0.5}Cd_{0.5}Ga_2S_4$
PACC: 7125T, 7120F, 4265K

1. Introduction

Mercury thiogallate $HgGa_2S_4$ (HGS) has been of considerable interest because of its nonlinear optical properties in the mid-infrared (mid-IR) spectral range, and the HGS crystal has a wide transparency range (from 0.5 to 13μm), high nonlinear susceptibility, and fairly good birefringence.[1−4] High values of laser damage threshold and conversion efficiency allow using the HGS crystal as frequency doubling and optical parametric oscillator (OPO)/ optical parametric amplifier (OPA) in the wavelength range from 1.0 to 10 μm.[5] For mid-IR OPO with Nd:YAG-laser pumping, the crystal HGS is optimal because it has favourable parameters, such as the value of effective nonlinear susceptibility, the transparent region and the value of absorption coefficient, the type of variance of principal values of refractive indices, potential optical quality and resistance to laser radiation.[6] Good nonlinear properties and optical quality of HGS allow this material to compete with $AgGaS_2$, $AgGaSe_2$, $ZnGeP_2$ and GaSe crystals, in spite of the considerable difficulty in growing big size crystals.[5] A HGS-based OPA pumped at 1kHz by a Cr:forsterite regenerative amplifier tuned to 1.25μm can be used to achieve a broad mid-IR tenability (5–9μm) of the idler.[7] The conversion efficiency of HGS is two times higher than that of argentum thiogallate ($AgGaS_2$) crystal.[6] In the literature, on the basis of chalcogenide crystals of $AgGaS_2$, HGS and $Hg_{1-x}Cd_xGa_2S_4$, the creation of powerful tunable mid- and far IR sources of light pulses is most practical.[6] It should be pointed out

*Project supported by the National Natural Science Foundation of China (Grant Nos 20373073 and 90201015), the Science Foundation of the Fujian Province, China (Grant Nos E0210028 and 2002F010), and the Foundation of State Key Laboratory of Structural Chemistry (Grant No 030060).

†E-mail: huangshp@fjirsm.ac.cn

that in HGS and $Hg_{1-x}Cd_xGa_2S_4$ crystals the parametric oscillation with pumping by the radiation of the second harmonic of the Nd:YAG-laser is possible because of specificity of refractive index variance in visible region.[4,8] Petrov and Rotermund experimentally demonstrated the superior properties of $Hg_{1-x}Cd_xGa_2S_4$ for frequency conversion of femtosecond pulses.[9] The mixed crystal $Hg_{1-x}Cd_xGa_2S_4$ can be used to generate the tunable narrow band cw laser radiation in the mid-IR for high-resolution and high-sensitivity spectroscopy and tailor the group-velocity mismatch to increase the interaction length for operation with ultrashort pulses in a nonlinear process, and to optimize the band gap so that a phase-matchable crystal can be pumped near 800 nm without the onset of two-photon absorption.[9]

In this paper, we will theoretically compare the optical properties between HGS and HCGS crystals, and describe an electronic origin of nonlinear optical response. At the same time, band structures and bond properties of these two crystals will be also discussed.

2. Computational procedures

HGS belongs to the defective chalcopyrite structure of AB_2C_4 type, as illustrated in Fig.1. Gallium atoms occupy the positions of two different types. The number of neighbouring atoms in the first atomic shell of the sulfur atom is three in this structure. The space group is $I(\bar{4})$-S_4^2, in which the sets of equivalent positions are: 2Hg (0 0 0); $2Ga^1$ (0 0 0.5); $2Ga^2$ (0 0.5 0.25); 8S(x y z) (x=0.2718; y=0.2675; z=0.1374).[3] Crystallographic data from Ref.[3] are used to optimize the parameters using the BFGS scheme[10] and Ultrasoft pseudopotentials[11,12] in CASTEP computer code.[13,14] And then the optimized structural parameters are used to calculate the electronic band structure and optical properties for HGS. The lattice constants and atom–atom distances obtained from Ref.[3] and the optimized structural parameters are listed in Table 1. To calculate the electronic band structure and optical properties of $Hg_{0.5}Cd_{0.5}Ga_2S_4$ (HCGS), we have chosen a 2×1×1 supercell which contains 28 atoms and partially substituted the element Hg by Cd in the A position of the AB_2C_4, and thus obtain HCGS. The structural parameters (lattice constants, bond angles, atomic coordinates etc) are optimized using the same method as that for HGS and the optimized structural parameters are listed in Table 2. From the optimized structural parameters, we can see that due to the effect of the substitution with Cd, the geometric structure is a little distorted from tetragonal, and it can be approximately regarded as tetragonal for HCGS. The periodic first-principles calculations presented here are based on density functional theory (DFT) using a plane-wave pseudopotential formalism and run by CASTEP program.[15] Computations are performed via nonlocal gradient-corrected functional designed by Perdew–Burke–Ernzerhof functional (GGA-PBE).[16] The norm-conserving pseudopotential developed by Lin *et al*[17] and Lee[18] was generated in the plane wave basis set to calculate the properties. The practical tools for applying DFT are the Kohn–Sham (KS) equations[19] in this study. Pseudo-atomic calculations are performed for S-$3s^23p^4$, Ga-$3d^{10}4s^24p^1$, Hg-$5d^{10}6s^2$ and for Cd-$4d^{10}5s^2$. A pseudopotential replaces both the atomic nucleus and the core electrons, i.e. a fixed effective potential that in a special sense reproduces the effect of the nuclear potential and the orthogonal requirement. The number of plane waves included in the basis is determined by a cutoff energy E_c of 590eV for both HGS and HCGS crystals. The convergent criterion of total energy is set to be 2.0×10^{-6}eV/atom. The Monkhorst–Pack k-point grid can be specified in a k-point separation way, and the separation is set to be 0.5nm^{-1} in the calculations.

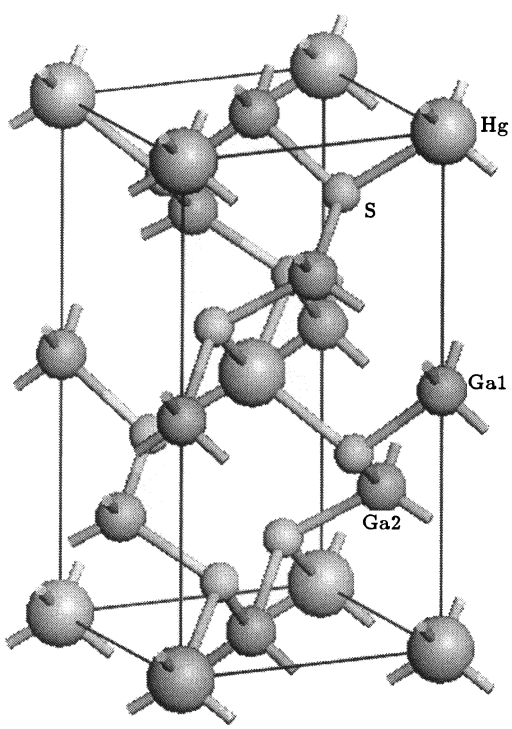


Fig.1. Unit cell of HGS.

Table 1. The lattice constants and atom–atom distances of HGS crystal.

	$a = b$/0.1nm	c/0.1nm	$\alpha = \beta = \gamma/(^\circ)$	Hg–S/0.1nm	Ga^1–S/0.1nm	Ga^2–S/0.1nm
Exp.[3]	5.5106	10.2392	90	2.52894	2.28082	2.28344
Cal.	5.701976	10.468655	90	2.60685	2.31190	2.31777

Table 2. The optimized lattice constants, atom–atom distances and bond population of HCGS crystal.

Optimized lattice constants				Bond	Average Population	Average Length/0.1nm
a	1.138181nm	α	90.00005°	Hg–S	0.435	2.60234
b	0.569090nm	β	90.00022°	Cd–S	0.465	2.57670
c	1.042286nm	γ	90.00036°	Ga–S	0.579	2.31005

The calculations of linear optical properties are made in terms of the complex dielectric function $\varepsilon = \varepsilon_1 + \mathrm{i}\varepsilon_2$. The imaginary part of the dielectric function, $\varepsilon_2(\omega)$, is given by[20]

$$\varepsilon_2(\omega) = 4(\pi e/m\omega)^2 \sum_{\mathrm{v,c}} \int_{\mathrm{BZ}} 2\mathrm{d}\boldsymbol{k}/(2\pi)^3 |e \cdot \boldsymbol{M}_{\mathrm{cv}}(k)|^2 \times \delta(E_{\mathrm{c}}(K) - E_{\mathrm{v}}(K) - \hbar\omega), \quad (1)$$

where $\sum$ denotes the summation over the valence bands (v) and conduction bands (c), and $\int$ the integration over $\boldsymbol{k}$ vectors in Brillouin zone (BZ). The $e \cdot \boldsymbol{M}_{\mathrm{cv}}(\boldsymbol{k})$ is an electron transition moment between the conduction and valence bands at $\boldsymbol{k}$ point, and the argument of the δ function is the energy difference between the conduction and valence bands at the $\boldsymbol{k}$ point with absorption of a quantum $\hbar\omega$, $(E_{\mathrm{c}}(K) - E_{\mathrm{v}}(K) - \hbar\omega)$. The calculation of $\varepsilon_2(\omega)$ includes 24 conduction bands in this study. $\varepsilon_2(\omega)$ can be considered as detailing the real transitions between occupied and unoccupied electronic states. Since the dielectric function describes a causal response, the real and imaginary parts are linked by a Kramers–Kronig transform. This transform is used to obtain the real part of the dielectric function, $\varepsilon_1(\omega)$.[21]

The first-order non-resonant susceptibility at low frequency region is given by $\chi^{(1)}(\omega)_{ii} = [\varepsilon(\omega)_{ii} - 1]/4\pi$. Furthermore, the second-order non-resonant susceptibility can be expressed in terms of the first-order susceptibilities as follows:[22]

$$\chi^{(2)}_{ijk}(-\omega_3; \omega_1, \omega_2) = F^{(2)} \chi^{(1)}_{ii}(\omega_3) \chi^{(1)}_{jj}(\omega_1) \chi^{(1)}_{kk}(\omega_2), \quad (2)$$

where $F^{(2)} = ma/(N^2 e^3)$. Equation (2) is derived from a classical anharmonic oscillator (AHO) model,[22] in which m and e are respectively electron mass and charge; a is a parameter that characterizes the nonlinearity of the response. The value of a can be obtained from experimental or theoretical estimations. It is noted that N is a density number of unit cells in a crystal instead of the density number of atoms in a classical AHO model.

3. Results and discussion

3.1. Band structures, density of states and chemical bonding

In order to have a good match between the calculated and experimental band gaps,[23] we employ a scissors operator[24,25] to calculate the band structures and density of states. The calculated band structures with a scissors operator of shift energy 1.0eV in the Brillouin zone are plotted in Figs.2(a) and (b) for HGS and HCGS, respectively, in which the Fermi level is set as energy reference. We expect that the band gap of HCGS is larger than that of HGS because an element Hg is replaced by a lighter element Cd. The electronic state energies at some k-points within the lowest conduction band (LCB) and the highest valence band (HVB) are listed in Table 3. The three numbers within brackets represent k-points along the three axes in reciprocal space. It is found that the lowest energy of conduction bands (CBs) and the highest energy of valence bands (VBs) for HGS and HCGS are both localized at G point, and they are described as direct-band-gap materials. The gaps are 2.55 and 2.80eV for HGS and HCGS, respectively. It is observed that the valence bands of both the crystals are flat while the conduction bands are oscillatory.

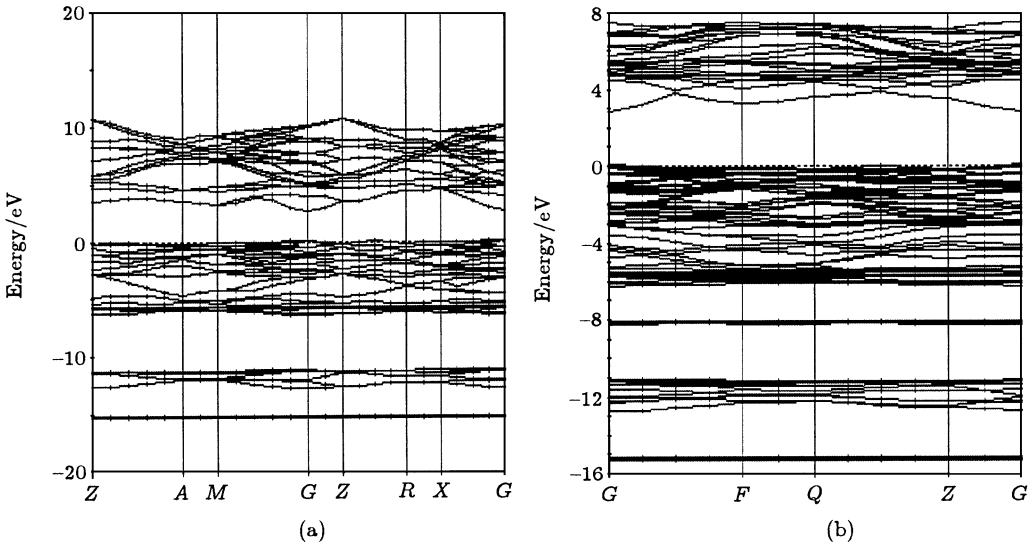


Fig.2. Energy band structures of (a) HGS, (b) HCGS.

Table 3. The state energies (eV) at some k-points of HGS and HCGS crystals.

Crystal	k-point	LCB	HVB	LCB-HVB
HGS	Z(0.0, 0.0, 0.5)	3.473793	−0.25674	3.730533
	A(0.5, 0.5, 0.5)	3.544484	−0.22891	3.773394
	M(0.5, 0.5, 0.0)	3.219521	−0.11029	3.329811
	G(0.0, 0.0, 0.0)	2.590018	0.040092	2.549926
HCGS	Z(0.0, 0.0, 0.5)	3.526815	−0.13924	3.666055
	F(0.0, 0.5, 0.0)	3.226484	−0.05890	3.285384
	Q(0.0, 0.5, 0.5)	3.580602	−0.13924	3.719842
	G(0.0, 0.0, 0.0)	2.845635	0.047879	2.797756

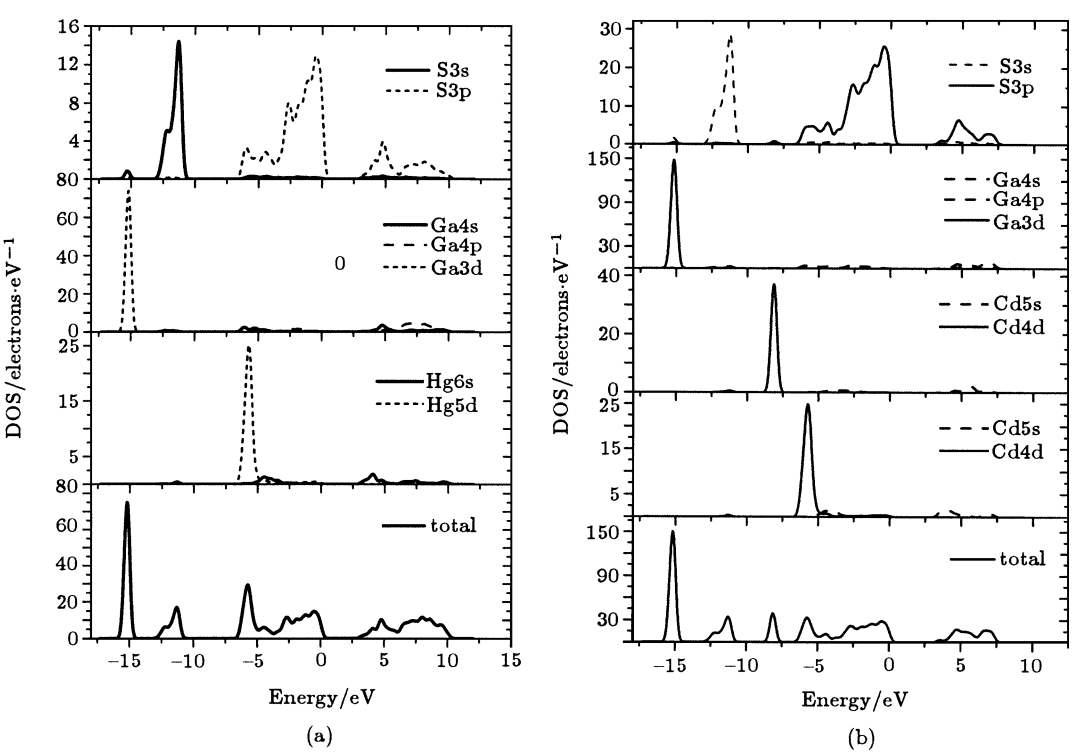


Fig.3. Total and partial density of states of crystals (a) HGS and (b) HCGS.

The bands can be assigned according to total and partial density of states (DOS), as plotted in Figs.3(a) and (b). The bands of both HGS and HCGS crystals lying around -15.0eV are mostly derived from the Ga-3d with a small mixing of S-3s states. The VBs ranging from –13.0 to –11.0eV mostly originate from S-3s for HGS and HCGS. Around -8.0eV, there are some bands derived from the Cd-4d, S-3s and S-3p states for HCGS. The Hg-5d, S-3p and Ga-4s states have contributions to the VBs between –7.0 and –5.0eV for both crystals. The top of VBs largely originates from the S-3p states with a small mixing of Hg-5d and Ga-4p states, and the bottom of CBs is mainly composed of S-3p and Ga-4s states with a small mixing of Hg-6s states for HGS. While for HCGS, the top of VBs mostly originates from the S-3p states and the bottom of CBs is mainly due to the Ga–S antibonding states.

Now, we elucidate the feature of chemical bonding from the nature of total DOS and angular momentum projected DOS (partial DOS). For the HGS crystal, we observe that the DOS, ranging from about -5.0 to 0.0eV, is larger for S-3p states (12.9electrons/eV) than for Ga-4p states (2.5electrons/eV) and for Hg-6s states (1.3electrons/eV), by comparing the total DOS with the angular momentum projected DOS of Hg-6s, Ga-4p and S-3p states as shown in Fig.3. These results show that some electrons from Hg-6s and Ga-4p states transfer into the VBs and take part in the substantial covalence interactions between Ga and S atoms and weak covalence interactions between Hg and S atoms. For the HCGS crystal, it is found that the DOS ranging from -5.0 to 0.0eV is larger for S-3p states (25.6electrons/eV) than for Ga-4p states (4.6electrons/eV), Cd-5s states (0.8electrons/eV) and Hg-6s states (1.4electrons/eV). This means that some electrons from Hg-6s, Cd-5s and Ga-4p states have transferred into the VBs and taken part in the weak covalence interactions between Hg and S atoms and between Cd and S atoms, and the substantial covalence interactions between Ga and S atoms, respectively. Here we note an interesting fact that the DOS of Ga and S atoms in HCGS is about two times that of the corresponding DOS of Ga and S atoms in HGS. The reason for this is that the supercell approach is used for the HCGS crystal in the calculations. The chemical bonding properties are also evidenced from the population analysis. The calculated bond orders for Hg–S and Ga^1–S, Ga^2–S bonds are 0.41, 0.53 and 0.56e in a unit cell of HGS respectively, and the Hg–S, Cd–S, Ga–S bonds lie in ranges from 0.43 to 0.44e, from 0.46 to 0.47e, from 0.56 to 0.60e respectively (the average bond population listed in Table 2) in a unit cell of HCGS (covalent single bond order is generally 1.0e). All the Hg–S and the Cd–S bonds in these two crystals are basically of ionic character, and the Ga–S bonds are of covalent character. Accordingly, we can also say that the covalent strength of Ga–S bonds is stronger than that of Hg–S (or Cd–S) bonds in both HGS and HCGS crystals.

3.2. Linear and nonlinear optical properties

The calculated imaginary $\varepsilon_2(\omega)$ and real $\varepsilon_1(\omega)$ parts of the dielectric function are shown respectively in Figs.4(a) and (b) for HGS and HCGS. The calculated imaginary part $\varepsilon_2(\omega)$ can be used to describe the real transitions between the occupied and unoccupied bands. It is found from dispersion of the $\varepsilon_2(\omega)$ spectra that the strongest absorption peak and cutoff edge of UV absorption are anisotropic. For HGS, the strongest absorption peaks are located at about

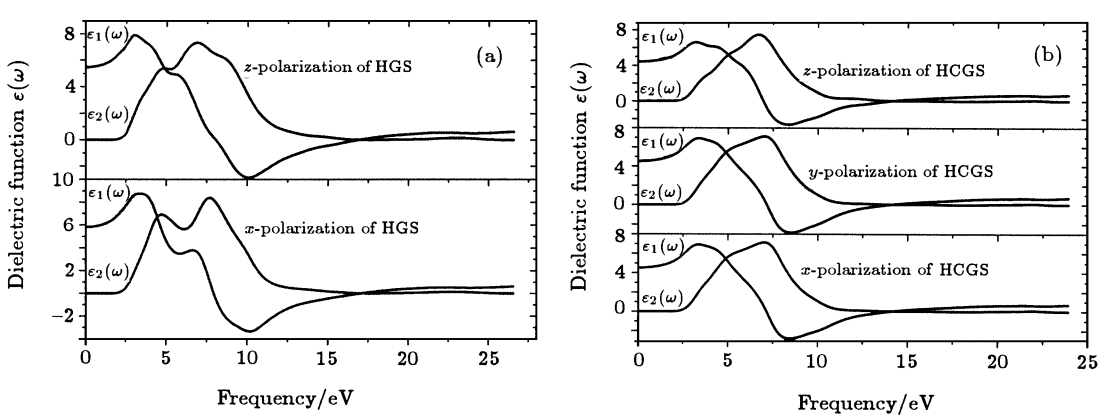


Fig.4. The calculated dielectric functions for (a) HGS, and (b) HCGS.

163.85nm (7.58eV) and 183.19nm (6.78eV) for a ($a = b$) and c axes, respectively. For HCGS, the strongest peaks are located at about 179.48nm (6.92eV) and 188.47nm (6.59eV) for a ($a \approx b$) and c axes, respectively. We can find that the absorption peaks and cutoff edges of UV absorption have a tendency to red-shift along a (or b) and c axial directions when some Hg atoms are replaced by Cd atoms in HGS. The real part $\varepsilon_1(\omega)$ can be used to describe the linear refractive index of the material at transmission region according to the relation $n^2(\omega) = \varepsilon(\omega) = \varepsilon_1(\omega) + i\varepsilon_2(\omega)$, because $\varepsilon_2(\omega)$ is nearly zero in the low-frequency zone. With a scissors operator of shift energy 1.0eV, the calculated refractive indices are in agreement with the experimental data for HGS[26], as shown in Fig.5. The calculated linear refractive indices from wavelengths of 1.0 to 8.0μm are plotted respectively in Figs.6(a) and (b) for HGS and HCGS. We can see that n^x is nearly equal to n^y for HCGS and it can be regarded as a quasi-uniaxial crystal ($n^x \approx n^y = n^{\rm o}$). The refractive index $n^{\rm o}$ is an ordinary refractive index which describes the refraction of light polarized perpendicular to the plane containing the propagation vector $\boldsymbol{k}$ and optic axis. The refractive index $n^{\rm e}$ is an extraordinary refractive index which describes the refraction of light polarized in the plane containing $\boldsymbol{k}$ and optic axis. It is found from Fig.6 that $n^{\rm e}$ is less than $n^{\rm o}$ for HGS and HCGS, and so HGS and HCGS are negative uniaxial crystals. The difference between $n^{\rm o}$ and $n^{\rm e}$ for HGS is larger than that for HCGS. It is known that the knowledge of refractive index of a material is necessary to predict its frequency-conversion properties in a device such as an optical parametric oscillator or a second-harmonic generator. Careful control of the refractive indices is required to establish the phase-matching condition for frequency-conversion devices.

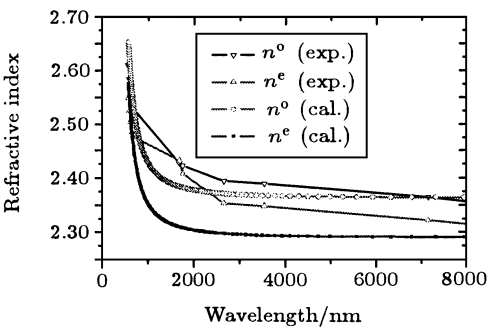


Fig.5. Calculated and experimental dispersion curves of the refractive indices of HGS.

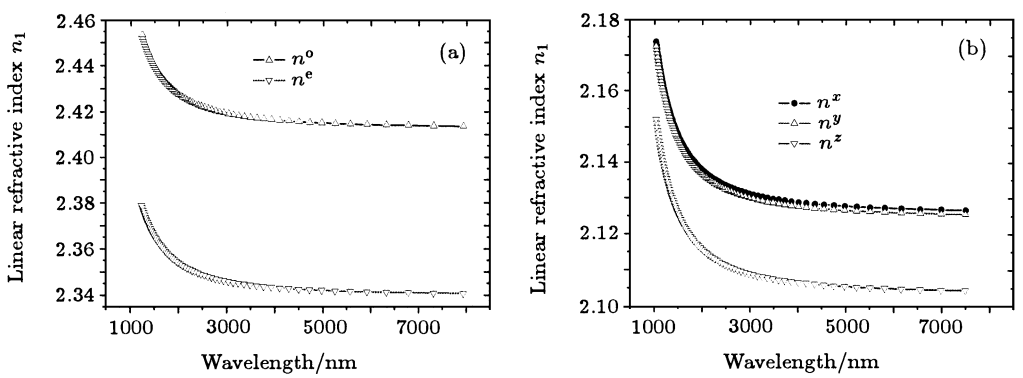


Fig.6. The calculated linear refractive indices of HGS (a) and HCGS (b).

The frequency-dependent second-order susceptibilities $\chi^{(2)}(-2\omega, \omega, \omega)_{312}$ and $\chi^{(2)}(-2\omega, \omega, \omega)_{311}$ are calculated using Eq.(2), and plotted in Fig.7 for HGS and HCGS. It is found that the susceptibilities $\chi^{(2)}(-2\omega, \omega, \omega)_{312}$ and $\chi^{(2)}(-2\omega, \omega, \omega)_{311}$ of HGS and HCGS are not significantly changed at above an incident wavelength of 2.5μm or below an input energy of 0.5eV. The calculated results for HGS crystal with a scissors operator of shift energy 1.0eV are in much closer agreement with the measured nonlinear optical constants d_{36} [$\chi^{(2)}(-2\omega, \omega, \omega)_{312} = 2d_{36}$] and d_{31}[$\chi^{(2)}(-2\omega, \omega, \omega)_{311} = 2d_{31}$] at the incident wavelengths of 1.064μm,[27] and 5.3μm.[28] The measured values of d_{36} and d_{31} at an input wavelength of 1.064μm are d_{36}=(35.2±5.3)pm/V, d_{31}=(11.7 ± 1.8)pm/V[27] and the measured values of d_{36} and d_{31} at the input wavelength of 5.3μm are d_{36} = 22.9pm/V, d_{31}=7.6pm/V.[28] Comparing Fig.7(a) with Fig.7(b), we find that d_{36} is larger than d_{31} by one order of magnitude for HGS. From Fig.7, we also see that the second-order susceptibility of HGS is larger than that of HCGS. This is due to the increase of the band

gap of the solid solution HCGS. Table 4 lists the second-order nonlinear optical parameters for HGS and HCGS crystals, and the calculated values of d_{36} and d_{31} show good agreement with the measured ones[27,28] for HGS.

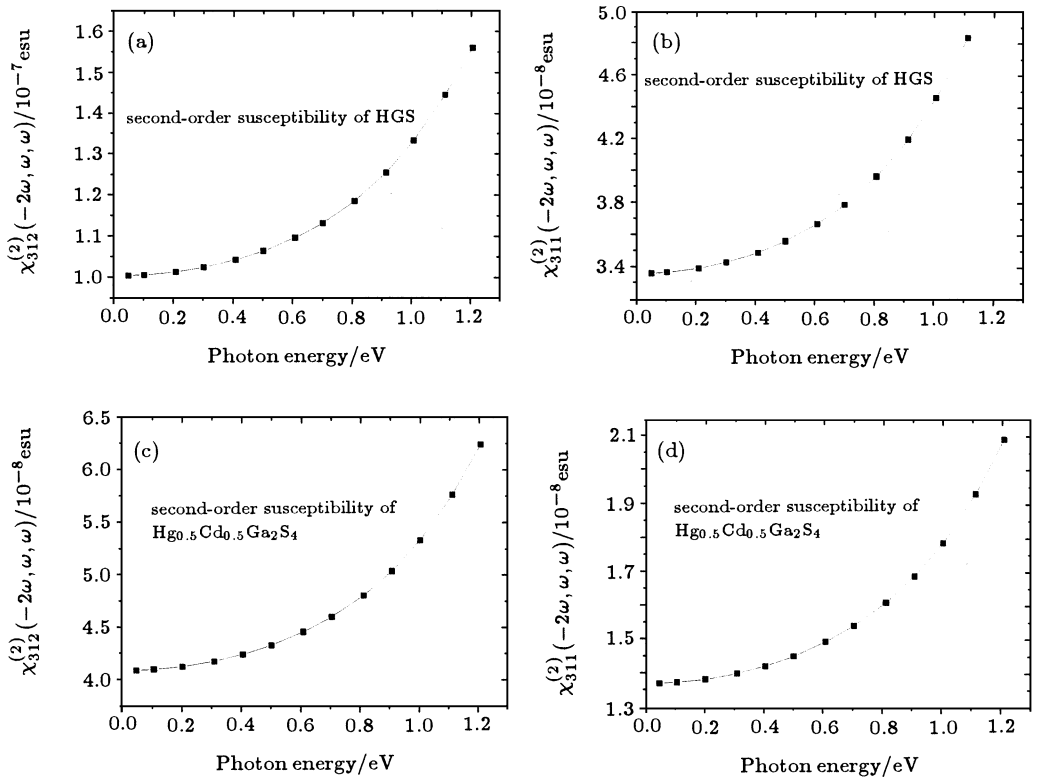


Fig.7. The calculated frequency-dependent second-order optical susceptibilities.

Table 4. The second-order optical parameters of HGS and HCGS crystals at an input wavelength of 1.064μm.

Crystal	$F^{(2)}/10^{-6}$esu	$\chi^{(2)}/10^{-7}$esu*	d_{il} of cal./(pm/V)	d_{il} of expt./(pm/V)
HGS	F_{zxy}=1.91	$\chi^{(2)}_{312}$=1.51	d_{36}=31.6	d_{36}=35.2 ± 5.3[27]
	F_{zxx}=0.639	$\chi^{(2)}_{311}$=0.506	d_{31}=10.6	d_{31}=11.7 ± 1.8
HCGS	F_{zxy}=1.91	$\chi^{(2)}_{312}$=0.604	d_{36}=12.7	
	F_{zxx}=0.639	$\chi^{(2)}_{311}$=0.202	d_{31}=4.23	

* $\chi = 2d$, and multiplying χ by 4.189×10^{-4} to obtain d in units of pm/V.

We can make three points by comparing the calculated and discussed results for HGS with those for HCGS: (A) the band gap of HGS is smaller than that of HCGS; (B) the optical susceptibilities of HGS are larger than those of HCGS; and (C) the refractive index of o-polarization is larger than that of e-polarization for both HGS and HCGS, and both are negative uniaxial crystals. We can explain point (A) by the partial substitution of the heavier element Hg by Cd. We note that Hg, a heavier element, has lower s-like states than Cd, and thus the replacement of Hg by Cd will make the gap larger.[29,30] As for point (B), we can explain it by the crystal lattice distortion and band structure variation. It is known that the susceptibility is proportional to the transition moments, and inversely proportional to the transition energies between VB and CB at a given k-point. The HGS and HCGS crystals both have the defective chalcopyrite structures, and there is not a very large difference between their transition moments which depend on geometric structure and charge. Accordingly, the difference between their susceptibilities depends on the energy band gap. It is shown from point (A) that the transition energy difference between CB and VB

is smaller for HGS than for HCGS. That is the reason why the HGS crystal has larger susceptibilities. For point (C), we have found that the sign of bond order difference δp ($\delta p = p_{\mathrm{AC}} - p_{\mathrm{BC}}$) determines the sign of a uniaxial crystal of chalcopyrite type. Here, the bond order of Hg–S or Cd–S is lower than that of Ga–S in the HGS and HCGS crystals and the bond order difference δp ($\delta p = p_{\mathrm{Hg-S}} - p_{\mathrm{Ga-S}} < 0.0$) is negative. Moreover, an origin of linear and nonlinear optical effects can be assigned in terms of band structure and DOS. As mentioned above, for HGS the top of VBs mostly originates from the S-3p states with a small mixing of Hg-5d and Ga-4p states, and the bottom of CBs is mainly due to the antibonding states between S-3p and Ga-4p orbitals. While for HCGS, the top of VBs mostly originates from the S-3p states and the bottom of CBs is mainly composed of the Ga–S antibonding states. Accordingly, charge transfer from S^{2-} to Ga^{3+} makes most contributions to optical effects for HGS and HCGS, and there are some influences upon linear and nonlinear optical responses by replacing Hg^{2+} by Cd^{2+} ions in HGS.

4. Conclusion

In summary, we have presented the electronic structures and optical properties of the HGS and HCGS crystals in terms of the calculated results using CASTEP code based on DFT. The atomic states contributing to the band structures have been assigned according to the total and partial DOS, and it has been shown that the top VBs are contributions from the Ga–S bonding states with small mixings of Hg–S bonding states, and the bottom of CBs mainly originates from S-3p and Ga-4s states with a small mixing of Hg-6s states for HGS. For the HCGS crystal, the top of VBs mostly originates from the S-3p states and the bottom of CBs is mainly due to the Ga–S antibonding states. By an analysis of bond charge distributions, all of the Hg–S and the Cd–S bonds in these two crystals are substantially of ionic character, and the Ga–S bonds are substantially of covalent character. Frequency-dependent first- and second-order optical properties have been discussed in terms of the calculated results by DFT combined with an anharmonic oscillator model. It has been found that the refractive index of o-polarization is larger than that of e-polarization for both the HGS and HCGS crystals, and the birefringence δn ($\delta n = n^{\mathrm{e}} - n^{\mathrm{o}}$) of HGS is larger than that of HCGS. The band gap of HGS is smaller than that of HCGS and the second-order susceptibilities of HGS are larger than those of HCGS. An electronic origin of linear and nonlinear optical effects mostly originates from the charge transfer from S^{2-} to Ga^{3+} for the HGS and HCGS crystals, and there are some influences on the susceptibilities by replacing Hg by Cd atoms in HGS crystal.

References

[1] Ursaki V V *et al* 2002 *J. Phys. Chem. Solids* **63** 1823
[2] Hahn H *et al* 1955 *Z. Anorg. Allg. Chem.* **279** 241
[3] Schwer H and Krämer V 1990 *Z. Kristallogr.* **190** 103
[4] Levine B F *et al* 1976 *IEEE J. Quantum Electron* **QE-12** 367
[5] Rotermund F, Petrov V and Noack F 2000 *Opt. Commun.* **185** 177
[6] Komarow A and Solomatin V S 1982 *Sov. Tech. Phys. Lett.* **8** 375
[7] Rotermund F and Petrov V 2000 *Opt. Lett.* **25** 746
[8] Petrov V *et al* 2004 *Opt. Commun.* **235** 219
[9] Petrov V and Rotermund F 2002 *Opt. Lett.* **27** 1705
[10] Fischer T H and Almlof J 1992 *J. Phys. Chem.* **96** 9768
[11] Vanderbilt D 1990 *Phys. Rev.* B **41** 7892
[12] Xu X G *et al* 2005 *Acta Phys. Sin.* **54** 0313
[13] Payne M C *et al* 1992 *Rev. Mod. Phys.* **64** 1045
[14] Segall M D *et al* 2002 *J. Phys.: Condens. Matter.* **14** 2717
[15] Materials Studio CASTEP version 3.0 Program developed by Accelrys Inc.
[16] Perdew J P, Burke K and Ernzerhof M 1996 *Phys. Rev. Lett.* **77** 3865
[17] Lin J S *et al* 1993 *Phys. Rev.* B **47** 4174
[18] Lee M H 1996 *PhD Thesis* (Cambridge University)
[19] Kohn W and Sham L J 1965 *Phys. Rev.* **140** (4A) A1133
[20] Bassani F and Parravicini G P 1975 *Electronic States and Optical Transitions in Solids* (Oxford: Pergamon) pp149–154
[21] Xu P S, Xie C K, Pan H B and Xu F Q 2004 *Chin. Phys.* **13** 2126
[22] Boyd R W 1992 *Nonlinear Optics* (New York: Academic) pp21–32
[23] MacKinnon A 1985 *Tables of Numerical Data and Functional Relationships in Science and Technology* (Berlin: Springer) Vol. 17 p124
[24] Godby R W, Schlüter M and Sham L J 1988 *Phys. Rev.* B **37** 10159
[25] Wang C S and Klein B M 1981 *Phys. Rev.* B **24** 3417
Hybertsen M S and Louie S G 1986 *Phys. Rev.* B **34** 5390
[26] Badikov V V *et al* 1979 *Sov. J. Quant. Electron.* **9** 1068
[27] Badikov V V *et al* 1980 *Sov. J. Quant. Electron.* **10** 1300
[28] Petrov V, Rotermund F and Noack F 2001 *J. Opt.* A **3** (3) R1
[29] Rashkeev S N, Limpijumnong S and Lambrecht W R L 1999 *Phys. Rev.* B **59** 2737
[30] Jiang X S and Lambrecht W R L 2004 *Phys. Rev.* B **69** 035201